HHS Public Access

Author manuscript

Dev Cell. Author manuscript; available in PMC 2016 September 28.

Published in final edited form as:

Dev Cell. 2015 September 28; 34(6): 682–693. doi:10.1016/j.devcel.2015.08.009.

A quality control mechanism removes unfit cells from a population of sporulating bacteria

Irene S. Tan[1,2], **Cordelia A. Weiss**[1], **David L. Popham**[3], and **Kumaran S. Ramamurthi**[1,*]

[1]Laboratory of Molecular Biology, National Cancer Institute, National Institutes of Health, Bethesda, MD, 20892, USA

[2]NIH-Johns Hopkins University Graduate Partnership Program, Baltimore, MD, 21218, USA

[3]Department of Biological Sciences, Virginia Tech, Blacksburg, VA 24061, USA

SUMMARY

Recent discoveries of regulated cell death in bacteria have led to speculation about possible benefits that apoptosis-like pathways may confer to single-celled organisms. However, establishing how these pathways provide increased ecological fitness has remained difficult to determine. Here, we report a pathway in *Bacillus subtilis* in which regulated cell death maintains the fidelity of sporulation through selective removal of cells that misassemble the spore envelope. The spore envelope, which protects the dormant spore's genome from environmental insults, uses the protein SpoIVA as a scaffold for assembly. We found that disrupting envelope assembly activates a cell death pathway wherein the small protein CmpA acts as an adaptor to the AAA+ ClpXP protease to degrade SpoIVA, thereby halting sporulation and resulting in lysis of defective sporulating cells. We propose that removal of unfit cells from a population of terminally differentiating cells protects against evolutionary deterioration, and ultimately loss, of the sporulation program.

Graphical Abstract

*Correspondence: ramamurthiks@mail.nih.gov.

AUTHOR CONTRIBUTIONS

Conceptualization, IST. and KSR.; Methodology, IST and KSR; Formal analysis, IST, CAW, DLP, and KSR.; Investigation, IST, CAW, DLP, and KSR; Writing-Original Draft, IST and KSR; Writing-Review and Editing, IST, CAW, DLP, and KSR; Funding Acquisition, DLP and KSR.

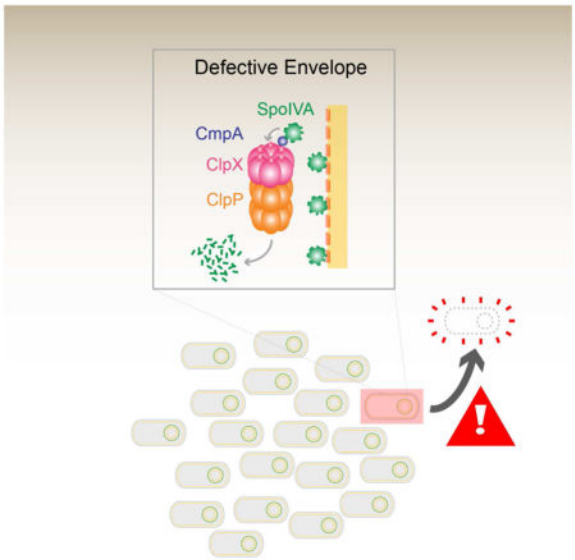

INTRODUCTION

Maintaining the fidelity of developmental programs is essential for ensuring the correct morphology of an organism. As such, key factors that determine morphogenesis are often subject to multiple layers of regulation. The alternative developmental pathway of bacterial endospore formation ("sporulation") provides a genetically tractable system to study cellular morphogenesis and mechanisms that maintain the robustness of differentiation programs (Higgins and Dworkin, 2012; Tan and Ramamurthi, 2014). In nutrient-rich conditions, the bacterium *Bacillus subtilis* divides symmetrically to yield two genetically and morphologically identical daughter cells. However, upon nutrient deprivation, *B. subtilis* initiates sporulation by dividing asymmetrically, resulting in two genetically identical, but morphologically distinct daughter cells (the larger "mother cell" and the smaller "forespore") that undergo different cell fates (Fig. 1A). Next, the mother cell engulfs the forespore; as a result, the forespore resides as a double membrane-bound cell within the mother cell. The forespore is then encased by the spore envelope which protects it from environmental insults and consists of two concentric shells whose assemblies are largely mediated by the mother cell (Henriques and Moran, 2007). The inner shell (the cortex) is made of a specialized peptidoglycan that assembles between the two membranes surrounding the forespore and eventually protects the spore from heat and helps maintain the dehydrated state of the spore core (Leggett et al., 2012; Popham et al., 1996). The outer shell (the coat) is composed of ~70 different proteins produced in the mother cell and is responsible for protecting the spore from chemical and enzymatic assaults (McKenney et al., 2013; Setlow, 2006). Ultimately, the mother cell lyses, thereby releasing the mature spore into the environment.

Assembly of the coat begins with the localization of a small 26-amino acid protein, SpoVM (Levin et al., 1993), which recognizes the outer forespore membrane by preferentially adsorbing onto the forespore's positively curved membrane surface (Gill et al., 2015; Ramamurthi et al., 2009). SpoVM recruits the structural protein SpoIVA (Price and Losick,

1999; Ramamurthi et al., 2006; Roels et al., 1992; Wu et al., 2015) which polymerizes irreversibly in an ATP-dependent manner around the forespore surface (Castaing et al., 2013; Ramamurthi and Losick, 2008). Deletion of either *spoVM* or *spoIVA* results in a misassembled coat that is not anchored to the forespore surface (Levin et al., 1993; Roels et al., 1992). Thus, SpoVM and SpoIVA are required for proper assembly of the basement layer, atop which other coat proteins are deposited (McKenney et al., 2010). Interestingly, deletion of *spoVM* or *spoIVA*, but not other major coat proteins, also abolishes assembly of the cortex (Levin et al., 1993; Roels et al., 1992) suggesting that SpoVM and SpoIVA play unique roles in orchestrating coat and cortex assembly.

Previously, we identified a small (37 codon) unannotated ORF in *B. subtilis* (which we termed "*cmpA*"), whose deletion suppressed the sporulation defect imposed by a mutant allele of *spoVM* that permitted initiation of coat assembly, but abrogated cortex assembly (Ebmeier et al., 2012). CmpA is produced in the mother cell during sporulation and overexpression of *cmpA* in wild type cells reduced sporulation efficiency. Whereas CmpA was degraded in wild type cells at a late stage of sporulation (when phase-bright forespores were elaborated), CmpA persisted in cells harboring the mutant allele of *spoVM*. We proposed that CmpA participates with SpoVM and SpoIVA in coordinating spore envelope assembly by inhibiting cortex assembly until coat assembly occurred, but the mechanism remained unclear. Here, we report that CmpA ensures proper envelope assembly by participating in a quality control pathway that selectively removes defective sporulating cells through regulated cell death to ultimately preserve the integrity of the sporulation program in the population. Using classical genetics we identified the AAA+ protease ClpXP (Baker and Sauer, 2012; Gottesman, 1996) as an additional participant in this pathway and propose that CmpA is an adaptor (Zhou et al., 2001) that delivers SpoIVA for degradation by ClpXP specifically in those cells in which the spore envelope has misassembled. Accordingly, we found that amino acid substitutions in CmpA, SpoIVA, or ClpX that disrupted complex formation led to restoration of SpoIVA stability in cells that had misassembled the spore envelope. We also found that deletion of *cmpA* permitted the completion of the sporulation program by cells harboring mutant alleles of *spoVM* and *spoIVA*, resulting in the formation of viable spores despite containing envelope assembly defects. We propose that CmpA persistence in mutant cells harboring an envelope defect promotes degradation of SpoIVA, which destabilizes the forespore and leads to cell lysis, thereby specifically removing defective cells and ensuring the fidelity of the sporulation program.

RESULTS

cmpA overexpression causes spore maturation defects and cell lysis

Overexpression of *cmpA* inhibits cortex assembly (Ebmeier et al., 2012), but the mechanism of inhibition remained unclear. To understand the impact of CmpA overproduction, we performed single-cell time lapse microscopy of wild type (WT) and *cmpA*-overexpressing (*cmpA*$^{++}$) cells (in which *cmpA* expression was driven by a constitutive promoter at an ectopic chromosomal locus) and monitored the fate of forespores that had achieved the phase bright state, an indicator of the spore core's dehydration (Imae and Strominger, 1976). Forespores in both WT and *cmpA*$^{++}$ cells progressed to the phase bright state. However,

while 74% (n=498) of WT phase bright forespores were ultimately released upon mother cell lysis during the monitoring period (Fig. 1B, arrowhead), in *cmpA*$^{++}$ cells 15% (n=222) of phase bright forespores were released and the remaining 85% relapsed to a phase-gray state (Fig. 1C, arrowhead), suggesting that they were largely unable to maintain core dehydration. In sporangia harboring relapsed phase-gray forespores, both mother cell and phase gray forespore lysed (Fig. 1D); additionally, released phase gray spores also ultimately lysed (Fig. 1E), suggesting that *cmpA* overexpression inhibited the cell's ability to maintain core dehydration, leading to cell lysis.

Since cell shape and osmotic stability are governed by cell wall integrity (Holtje, 1998), we next examined the effect of *cmpA*-overexpression on cortex peptidoglycan (PG) levels and composition. We harvested soluble PG precursors and assembled PG from WT and *cmpA*$^{++}$ cells at various time points during sporulation. Both strains initially (~t_0–t_8) accumulated soluble PG precursors, and depleted this pool coincident with cortex assembly (Fig. S1). During this initial period, both strains also accumulated assembled PG, indicating that cortex assembly was occurring normally (Fig. 1F). WT cells subsequently maintained steady levels of assembled PG after t_8 (the slight reduction after t_8 is due to mother cell lysis upon completion of sporulation), indicating the presence of a stable cortex. However, recovered PG from *cmpA*$^{++}$ cells decreased after t_8 (Fig. 1F), presumably due to an inability to harvest cells that lysed (Fig. 1D–E). To confirm that *cmpA*$^{++}$ cells were lysing we monitored the optical density (OD_{600}) of sporulating *cmpA*$^{++}$ cultures. In sporulation medium, OD_{600} of WT cultures increased; upon stationary phase (~t_6), OD_{600} remained roughly constant, after a transient decrease coincident with the entry into sporulation (Fig. 1G). In contrast, OD_{600} of *cmpA*$^{++}$ cultures initially increased in density similar to WT, but decreased in stationary phase, indicative of cell lysis (Fig. 1G).

Consistent with a defect in cortex maintenance, we observed that *cmpA*$^{++}$ sporangia did not accumulate dipicolinic acid (DPA; Fig. 1H), a small molecule that displaces water and is required for core dehydration (Paidhungat et al., 2000). Interestingly, the inability to maintain a stable cortex after normal initial assembly and the inability to accumulate DPA of *cmpA*$^{++}$ cells was reminiscent of the phenotypes associated with a *spoIVA* cortex-deficient point mutant (Catalano et al., 2001), suggesting that *cmpA*$^{++}$ is abrogating *spoIVA*'s cortex assembly function.

Two mechanisms could possibly contribute to the instability of the assembled cortex PG: (*1*) mechanical instability of the cortex due to defective envelope assembly, or (*2*) premature activation of cortex lytic hydrolases that degrade the cortex during germination. To rule out the second scenario, we deleted *sleB* and *cwlJ*, which encode the two known germination cortex lytic hydrolases (Heffron et al., 2009), and measured sporulation efficiency. Deletion of *sleB* and *cwlJ* did not suppress the *cmpA*$^{++}$ sporulation defect (Table S1, Strain D) indicating that *cmpA's* inhibition of cortex maturation is not due to premature germination, and instead suggesting that *cmpA*$^{++}$ prevents the maintenance of a stable cortex.

To determine if cell lysis caused by *cmpA*$^{++}$ is mediated by factors involved in the programmed mother cell lysis that releases the mature spore, we examined sporulation efficiencies of *cmpA*$^{++}$ cells in the absence of the three known sporulation-specific cell wall

hydrolases. *cmpA*$^{++}$ cells exhibited an almost 200-fold decrease in sporulation efficiency (Table S2, Strain B), while Δ*cwlC*, Δ*cwlH*, Δ*lytC*, and Δ*lytC* Δ*cwlC* cells (Smith and Foster, 1995) sporulated similarly to WT (Table S2, Strains C, E, G, I). However, deletion of *cwlC*, *cwlH*, *lytC*, or *lytC* and *cwlC*, did not rescue the sporulation defect imposed by CmpA overproduction (Table S2, Strains D, F, H, J), suggesting that CmpA-mediated lysis and cortex inhibition is largely independent of known enzymes involved in programmed mother cell lysis.

Identification of other factors interacting with CmpA

To understand how CmpA inhibits cortex stability we sought to identify other factors that participate in this pathway. Deletion of *cmpA* was identified as an extragenic suppressor of the cortex-deficient *spoVM*^{I15A} allele, and CmpA abnormally persisted late into sporulation in the *spoVM*^{I15A} mutant (Ebmeier et al., 2012). We therefore selected for additional suppressors that corrected the *spoVM*^{I15A} sporulation defect. To prevent isolating *cmpA* null mutations, we performed the selection in a strain harboring two chromosomal copies of *cmpA*. Two of the suppressors mapped to *spoIVA* (Table S3, Strain C and D). The first changed Glu423 to Gly, and the second changed Leu424 to Phe. The proximity of these two substitutions indicated that this region of SpoIVA may be important for interacting with CmpA or SpoVM and suggested that SpoVM, SpoIVA and CmpA participate together to orchestrate coat and cortex assembly.

We previously reported that proper localization of the largely functional CmpA-GFP is directly or indirectly dependent on *spoVM* [(Ebmeier et al., 2012); Fig. 2B)]; however, the mislocalization phenotype in the absence of SpoVM (increased CmpA-GFP accumulation as a focus on the forespore, reminiscent of the mislocalization phenotype of GFP-SpoIVA in the absence of SpoVM; Fig. 2B, arrowhead), together with the isolation of suppressor mutations in *spoIVA*, suggested that SpoIVA may be interacting with CmpA. Accordingly, in the absence of SpoIVA or SpoIVA and SpoVM, we found that CmpA-GFP was principally mislocalized in the mother cell cytosol (Fig. 2C–D), suggesting that SpoIVA is the major localization determinant for CmpA.

Next, we exploited the heat sensitivity caused by *cmpA* overexpression (Table S4) to select for suppressors that would correct this phenotype. This selection yielded four suppressors. Three suppressors mapped to *clpX*, which encodes the ATPase subunit of the ClpXP protease [(Gottesman et al., 1993; Wojtkowiak et al., 1993); Table S3, Strains C–E]. All three suppressors (D21Y, I34M, and E44G) resulted in N-terminal substitutions in ClpX, the domain implicated in substrate binding (Wojtyra et al., 2003). A fourth suppressor mapped to *clpP*, which encodes the proteolytic subunit of ClpXP (Table S4, Strain F). This mutation changed Asp187 to Asn near the hydrophobic pocket of ClpP that interacts with the “IGF loop” of ClpX (Kim et al., 2001), thereby possibly affecting interactions between ClpX and ClpP.

ClpX is required for entry into sporulation [(Liu et al., 1999); Table S5, strain B], and overproduction of ClpX did not significantly affect sporulation (Table S5, strain E). However, co-overproduction of ClpX and CmpA resulted in a sporulation efficiency of 7.6×10^{-5} relative to WT (Table S5, strain G), which was worse than the ~200-fold defect caused

by overproduction of CmpA alone (Table S5, strain C). To test if suppression by the *clpX* mutations were due to a loss of function, we deleted the N-terminus of ClpX and determined whether it suppressed the *cmpA*$^{++}$ defect. Cells overproducing ClpX$^{\Delta 1\text{-}53}$ (the endogenous copy of *clpX* was present in this strain to ensure entry into sporulation) and CmpA sporulated at near WT levels (Table S5, strain I), suggesting that the suppressor mutations decreased a function of ClpX's N-terminus. We conclude that the loss of ClpX's ability to bind a substrate overcomes the sporulation defect imposed by CmpA overproduction.

In addition to being the ATPase subunit of ClpXP protease, ClpX can function alone as a folding chaperone for some substrates (Schirmer et al., 1996). To test if the *clpP*^{D187N} suppressor was a loss-of-function mutation, we constructed a ClpX^{F270W} variant, which disrupts the IGF loop and diminishes ClpX interaction with ClpP (Kim et al., 2001). Similar to ClpX$^{\Delta 1\text{-}53}$, co-overproduction of ClpX^{F270W} with CmpA restored sporulation efficiency to near WT levels (Table S5, strain I), suggesting that abrogating the interaction between ClpX and ClpP corrects the *cmpA*$^{++}$ defect. Taken together, the genetic data are consistent with a model in which binding and degradation of one or more substrates by ClpXP is responsible for the sporulation defect imposed by CmpA overproduction.

CmpA is a ClpXP adaptor for binding SpoIVA

Since CmpA overproduction inhibited cortex maturation and ClpX acted synergistically with CmpA to inhibit sporulation (Table S5, Strain G), we hypothesized that CmpA is an adaptor that delivers a protein required for cortex maturation to ClpXP for degradation. To isolate a nonfunctional CmpA variant for use as a negative control, we performed alanine scanning mutagenesis of the 37 codon *cmpA* ORF, monitored the subcellular localization of the resulting variants fused to GFP (Fig. S2) and assessed each variant's function by measuring their ability to suppress the *spoVM*^{I15A} sporulation defect (Table S6). In the presence of *cmpA*^{P2A}, cells harboring *spoVM*^{I15A} sporulated similarly to cells harboring Δ*cmpA* (Table S6, row 4, strain IT139), suggesting that substitution of Pro2 with Ala abolished CmpA function. Nonetheless, CmpA^{P2A}-GFP localized properly to the forespore surface (Fig. S2).

To test if CmpA and ClpX interact we produced ClpX harboring a C-terminal His_6 tag. To promote stabilization of the hexameric form of ClpX that would bind adaptors and substrates, but would be unable to degrade bound substrates, we introduced a substitution (E182A) in ClpX's Walker B motif that disrupts ATP hydrolysis, but not ATP binding (Baker and Sauer, 2012). We then overproduced ClpX^{E182A}-His_6 (hereafter, simply ClpX-His_6) in cells that also produced low levels of WT ClpX to enable entry into sporulation. Next, we purified ClpX-His_6 from vegetative or sporulating cells that also produced CmpA-GFP or CmpA^{P2A}-GFP (Fig. 3). In vegetative cells, CmpA-GFP, but not CmpA^{P2A}-GFP, co-purified with ClpX-His_6 (Fig. 3A). We next purified ClpX^{I134M}-His_6 (also harboring a Walker B disruption) from vegetative cells that produced CmpA-GFP. Whereas ClpX-His_6 co-purified with CmpA-GFP, the amount of CmpA-GFP that co-purified with ClpX^{I34M}-His_6 was diminished (Fig. 3B). Together, the data indicated that ClpX and CmpA interact in the absence of sporulation factors in a manner requiring Pro2 of CmpA and Ile34 of ClpX.

We next wondered if SpoIVA would bind to ClpX and CmpA. In sporulating cells, SpoIVA co-purified with ClpX-His$_6$ and CmpA-GFP, but not in the presence of CmpA^{P2A}-GFP (Fig. 3C). Additionally, while SpoIVA co-purified with ClpX-His$_6$, SpoIVA did not co-purify with ClpX^{I134M}-His$_6$ (Fig. 3D). Further, whereas SpoIVA co-purified with ClpX-His$_6$ and CmpA-GFP, SpoIVA^{L424F} did not (Fig. 3E). Consistent with the results from the co-purification performed in vegetative cells (Fig. 3A), CmpA-GFP co-purified with ClpX-His$_6$ even in the presence of SpoIVA^{L424F} (Fig. 3E). Finally, to test if all three proteins exist in a single complex, we repeated the co-purification experiment with the affinity tag placed on CmpA-GFP. In sporulating cells producing low levels of ClpX and overproducing ClpX^{E182A}, purification of CmpA-GFP-His$_6$, but not CmpA^{P2A}-GFP-His$_6$, led to the co-purification of ClpX and SpoIVA (Fig. 3F). Taken together, we conclude that ClpX, CmpA, and SpoIVA form a complex, SpoIVA is not required for ClpX-CmpA interaction, and disruption of the N-terminal substrate binding domain of ClpX, Pro2 in CmpA, or Leu424 in SpoIVA abolishes formation of the ternary complex (Fig. 3G). The data thus far are consistent with a model in which CmpA delivers SpoIVA to ClpXP for degradation.

Spore envelope defects cause CmpA-driven SpoIVA degradation

To test if SpoIVA is a substrate for degradation by ClpXP, we examined the steady state levels of SpoIVA by immunoblotting cell extracts harvested from cells containing *spoVM*^{I15A}, which activates the CmpA pathway. SpoIVA was detected in WT cells at $t_{3.5}$ of sporulation, and similar levels of SpoIVA were maintained through $t_{5.5}$ (Fig. 4A–B). In the presence of *spoVM*^{I15A}, SpoIVA levels rapidly diminished by $t_{5.5}$, but SpoIVA levels were restored upon *cmpA* deletion, even in the presence of *spoVM*^{I15A} (Fig. 4A–B). To test if the decrease in SpoIVA levels was due to degradation, we inhibited translation by addition of spectinomycin and measured SpoIVA levels. Whereas WT strains maintained steady levels of synthesized SpoIVA even 2 h after inhibition of translation, in strains expressing *spoVM*^{I15A} SpoIVA was rapidly depleted and almost undetectable after 2 h (Fig. 4C–D). Deletion of *cmpA*, though, prevented depletion of SpoIVA in cells expressing *spoVM*^{I15A}, suggesting that in cells harboring mutations causing spore envelope defects (e.g. *spoVM*^{I15A}) SpoIVA is degraded in a CmpA-dependent manner.

To determine if SpoIVA is degraded in a particular subpopulation of sporulating cells, we examined the stability of GFP-SpoIVA in cells expressing *spoVM*^{I15A} using fluorescence microscopy (Fig. 5A–K). At $t_{3.5}$ of sporulation, localization and levels of GFP-SpoIVA were similar in WT and *spoVM*^{I15A} cells (Fig. 5A–B). At $t_{5.5}$, when most sporangia had elaborated a phase-bright forespore, WT cells maintained similar amounts of GFP-SpoIVA (Fig. 5F, 5K), but in the presence of *spoVM*^{I15A}, sporangia containing a phase-bright forespore were largely devoid of GFP-SpoIVA (Fig. 5G, 5K). When *cmpA* was deleted, GFP-SpoIVA levels returned to near WT levels despite the presence of *spoVM*^{I15A} (Fig. 5H, 5K). We then reasoned that disruption of the CmpA-ClpX-SpoIVA complex through the use of the *clpX* point mutants should also restore SpoIVA stability at $t_{5.5}$ and found that this was the case (Fig. 5D–E, I–K).

We also examined the persistence of GFP-SpoIVA^{L424F} (Fig. 5L–R), with the expectation that it would be resistant to degradation since it did not bind to ClpX (Fig. 3E). In WT cells

GFP-SpoIVA^{L424F} behaved similarly to GFP-SpoIVA in its localization to the forespore and persistence in phase bright forespores (Fig. 5L, 5R). In the presence of *spoVM*^{I15A} and *spoIVA* at the native locus, GFP-SpoIVA^{L424F} was degraded (Fig. 5P, 5R), but when the native locus harbored *spoIVA*^{L424F} instead, GFP-SpoIVA^{L424F} was largely resistant to degradation (Fig. 5Q, 5R). The recessive nature of the *spoIVA*^{L424F} allele may be explained by the ability of SpoIVA to polymerize (Ramamurthi and Losick, 2008), whereby SpoIVA that are degraded in a CmpA-dependent manner could recruit interacting SpoIVA^{L424F} molecules to ClpX that would not otherwise bind to CmpA and be subject to degradation. We conclude that SpoIVA is degraded in a CmpA-dependent manner in cells harboring a mutation (e.g. *spoVM*^{I15A}) that causes improper spore envelope assembly.

Additional factors under σ^K control are required for degradation of SpoIVA and CmpA

Our observation that degradation of GFP-SpoIVA only occurred in cells that had reached the phase bright forespore state led us to wonder whether some factor was preventing degradation at an earlier time point or if an additional factor was required for SpoIVA degradation at a later time point. We therefore overproduced CmpA and ClpX at an early time point (t_3 of sporulation), added spectinomycin after 15 min to prevent further translation, and monitored SpoIVA levels and observed no significant degradation of SpoIVA (Fig. S3), indicating that ClpX and CmpA were not sufficient for SpoIVA degradation. The appearance of phase bright spores is coincident with activation of the mother cell-specific sigma factor, σ^K, so we wondered whether the additional factor(s) were produced by σ^K. If so, we would expect GFP-SpoIVA degradation to be inhibited by preventing σ^K activation. Thus, we monitored GFP-SpoIVA levels in sporulating cells harboring a deletion in *spoIVCA*, which is required for producing functional σ^K (Kunkel et al., 1990). At an early time point, GFP-SpoIVA stability and localization were similar in WT cells and in cells harboring *spoVM*^{I15A} in the absence of σ^K (Fig. 6A, B). However, at a later time point, the absence of σ^K prevented degradation of GFP-SpoIVA in phase-bright forespores of the *spoVM*^{I15A} mutant (Fig. 6D) suggesting that at least one factor produced by σ^K is required for CmpA/ClpXP-mediated degradation of SpoIVA.

Since CmpA-GFP is also degraded specifically in WT cells elaborating phase bright forespores (Ebmeier et al., 2012) we next tested if CmpA-GFP stability was affected by the absence of σ^K. We induced *cmpA-gfp* expression at t_3 of sporulation; at $t_{3.5}$ CmpA-GFP localized to the forespore in all tested strains (Fig. 6E–H). At $t_{5.5}$, CmpA-GFP was no longer detectable in WT cells containing a phase-bright forespore (Fig. 6I), but persisted in the *spoVM*^{I15A} mutant [(Ebmeier et al., 2012); Fig. 6J]. In the absence of σ^K, CmpA-GFP persisted not only in cells harboring *spoVM*^{I15A} (Fig. 6L), but also in WT cells that elaborated phase bright forespores (Fig. 6K), indicating that degradation of CmpA requires a factor under the control of σ^K. The data suggest that σ^K controls two parts of the pathway. In WT cells that have successfully initiated spore envelope assembly, σ^K directs CmpA degradation so that sporulation may proceed. In cells that are unable to initiate spore envelope assembly, at least one additional factor produced under control of σ^K is required for CmpA/ClpXP-mediated degradation of SpoIVA.

CmpA is part of a quality control mechanism that maintains the integrity of a sporulating population

To determine if CmpA participates in a quality control mechanism that removes cells harboring incorrectly assembled spore envelopes from the population, we examined if deletion of *cmpA* would permit cells harboring other spore envelope defects to proceed past this checkpoint. To this end, we investigated the effect of *cmpA* deletion on a *spoVM*^{K2A} mutant that behaves similarly to the *spoVM*^{I15A} mutant (Fig. S4). Cells harboring *spoVM*^{K2A} produced ~100-fold fewer heat resistant spores and ~150-fold fewer lysozyme resistant spores relative to WT cells (Table 1, Strain B), but deletion of *cmpA* suppressed these defects (Table 1, Strain C). Sporangia harboring SpoIVA variants that fail to polymerize, either due to an inability to bind (SpoIVA^{K30A}) or hydrolyze (SpoIVA$^{T70A\text{-}T71A}$) ATP, do not assemble a coat and produce 10^4–10^6-fold fewer heat resistant spores than WT (Table 1, Strains F and H). Although deletion of *cmpA* did not suppress the sporulation defect of Δ*spoIVA* [and so is unable to bypass the requirement for SpoIVA altogether (Table 1, Strains J–K)] Δ*cmpA* suppressed the polymerization-defective *spoIVA* alleles, raising the sporulation efficiency (heat resistance) ~200–3000 -fold (Table 1, Strains G and I). Δ*cmpA* also partially suppressed the lysozyme sensitivity of these mutants, indicating that some coat assembly was permitted to occur (Table 1, Strains G and I).

To test if the presence of CmpA in cells harboring envelope defects resulted in the production of fewer viable spores, or a high level of viable, but heat sensitive, spores, we determined the total viable spore count for cells containing *spoVM*^{I15A} or *spoIVA*$^{T70A\text{-}T71A}$ in the presence and absence of CmpA by isolating viable spores by gradient centrifugation, then subjecting them to high heat. Cells harboring *spoVM*^{I15A} produced just 347 ± 141 viable spores ml^{-1}, compared to $8.6 \times 10^7 \pm 4.1 \times 10^7$ spores ml^{-1} produced by WT, of which 79% and 44%, respectively, were heat resistant (Table S7, strains A–B). Deletion of *cmpA* in cells harboring *spoVM*^{I15A} resulted in the production of $6.1 \times 10^6 \pm 4.0 \times 10^6$ spores ml^{-1}, of which nearly half were heat resistant (Table S7, strain C). Similar results were obtained in the suppression of the *spoIVA*$^{T70A\text{-}T71A}$ allele by deletion of *cmpA* (Table S7, strains D–E). Taken together, we conclude that deletion of *cmpA* allows mutants harboring spore envelope defects to bypass a quality control checkpoint, escape cell lysis, and continue with sporulation to produce large quantities of viable spores leading to the persistence and propagation of such mutations in the population. In contrast, the presence of CmpA in envelope-defective cells prevents completion of the sporulation program and removes those cells from the population.

DISCUSSION

The use of checkpoints ensures that steps in a developmental program properly finish prior to progression into the next stage of the program (Hartwell and Weinert, 1989). Here, we discovered that, during sporulation in *B. subtilis*, the small protein CmpA participates with the ClpXP proteolytic machinery in a quality control checkpoint during a terminal differentiation program to monitor proper spore envelope assembly. We propose a model (Fig. 6O) in which CmpA is an adaptor to ClpXP to mediate the degradation of the coat morphogenetic protein SpoIVA specifically in cells that improperly assemble the spore

envelope. Degradation of SpoIVA is linked to destabilization of defective sporangia and ultimately results in their lysis, thereby removing defective spores from the population. In cells that properly construct the spore envelope, degradation of CmpA signals successful spore envelope assembly and prevents SpoIVA proteolysis, permitting these cells to continue through the sporulation program. The model suggests that deleting *cmpA*, or disrupting the interactions between CmpA, ClpXP, and SpoIVA bypasses the checkpoint and permits mutant cells elaborating defective spore envelopes to continue through the sporulation program and persist in the population.

Our model is consistent with several lines of genetic, biochemical, and cytological evidence. Disruption of sporulation by overexpression of *cmpA* was suppressed by three different loss-of-function mutations in *clpX* that changed residues in the substrate and adaptor-binding N-terminus of ClpX. A fourth spontaneous mutation in *clpP*, that altered a residue near the hydrophobic binding pocket that mediates ClpP's interaction with ClpX, also suppressed the sporulation defect caused by *cmpA* overexpression. Involvement of SpoIVA as a target for degradation by ClpXP arose from two mutations in adjacent codons of *spoIVA* that altered residues between the Middle and C-terminal domain of SpoIVA (Castaing et al., 2014), suppressed the sporulation defect of the $spoVM^{I15A}$ allele (which arrests sporulation in a CmpA-dependent manner) and led to stabilization of SpoIVA.

Biochemical support for the model came from co-purification experiments which showed that CmpA, ClpX, and SpoIVA can exist in complex. Consistent with our genetic data, amino acid substitutions in CmpA, ClpX, or SpoIVA that bypassed the CmpA checkpoint *in vivo* also failed to form the ternary complex *in vitro*. We also found that CmpA interacts with the N-terminus of ClpX, and that this interaction can occur in the absence of SpoIVA. However, the interaction between SpoIVA and ClpX absolutely required CmpA. Together, this behavior is consistent with an adaptor-like function for CmpA, similar to that which has been described for ClpXP adaptors in other systems (Battesti and Gottesman, 2013).

Finally, epifluorescence microscopy of individual cells revealed that degradation of GFP-SpoIVA occurred specifically in mutant cells that had progressed to the phase bright forespore state, which is the stage in sporulation at which CmpA-GFP abnormally persists in the $spoVM^{I15A}$ mutant. However, disrupting CmpA/ClpX/SpoIVA complex formation in envelope-assembly mutants resulted in persistence of GFP-SpoIVA, completion of the sporulation program, and production of high levels of viable spores. The eventual disappearance of CmpA-GFP in in WT cells suggests that regulation of the checkpoint may be controlled via degradation of CmpA. Unlike other early-acting sporulation checkpoints that monitor ploidy, or fidelity and translocation of the genome prior to commitment to the onset of sporulation (Bejerano-Sagie et al., 2006; Burkholder et al., 2001; Fiche et al., 2013; Veening et al., 2009), CmpA is part of a late stage quality control mechanism that monitors the integrity of the developing spore. In this pathway, we propose that spore envelope defects arising at a late stage (so-called "Stage IV–V") result in lysis of the sporangium linked to SpoIVA degradation by CmpA and ClpXP. Consistent with this timing, we also report that the switch to initiate this pathway resides under control of σ^K, the final compartment-specific sporulation sigma factor which is also required for activating cortex synthesis (Vasudevan et al., 2007). We found that at least one unidentified factor produced

by σ^K is required to activate CmpA/ClpXP-mediated degradation of SpoIVA in mutant cells, and that σ^K is required for degradation of CmpA in properly sporulating cells. It is possible that the additional factor required for SpoIVA degradation is responsible for a post-translational modification of SpoIVA that marks it as a substrate for degradation by CmpA/ClpXP, or that recruitment of SpoIVA to ClpXP requires a second factor, in addition to CmpA (Lau et al., 2015).

We previously reported that Δ*cmpA* cells attain heat resistance slightly faster than WT (Ebmeier et al., 2012), suggesting that CmpA may perform a still poorly-defined role in slowing down the sporulation program, perhaps to ensure that proper spore envelope assembly occurs before the cell moves on to subsequent steps. In this report, we demonstrate that CmpA also acts upon mutant cells that fail to elaborate a proper envelope, and removes them from the population entirely. In this capacity, we propose that sporulating cells provide a window between σ^E and σ^K activation for the spore envelope to initiate assembly properly. Upon σ^K activation, if the spore envelope has properly assembled, the cell degrades CmpA and sporulation proceeds. However, if the envelope improperly assembles, CmpA instead persists, SpoIVA is degraded, and the cell lyses. Since SpoIVA and SpoVM are the only coat proteins that are also required for cortex assembly (heat resistance), it is appropriate that targeting a single protein, SpoIVA, for regulated degradation may result in destabilization of the entire spore envelope.

Recent reports of “apoptotic-like” cell death in bacterial cells have added to the changing view of bacterial communities as more than simply a collection of independently operating cells, leading to speculation that unicellular organisms may initiate cell death to benefit the population as a whole (Bos et al., 2012; Dwyer et al., 2012; McFarland et al., 2015). Although specific mechanisms for cell death in these cases have been well characterized, the exact benefit of such an act to a single-celled organism has sometimes been difficult to explicitly demonstrate. The use of the term “apoptosis” in bacteria has therefore remained controversial (Galluzzi et al., 2012; Hacker, 2013). Unlike regulated cell death pathways described in actively dividing cells, the CmpA pathway functions during a terminal differentiation program that produces a spore, a specialized cell type that preserves the cell’s genetic material in a manner functionally similar to that of germ cells in multicellular organisms. The construction of an envelope that is resistant to environmental insults is critical for the spore’s survival in harsh environmental conditions. As such, removal of cells harboring mutations that produce defective spore envelopes confers an obvious advantage to a population that needs to protect the integrity of its germ line’s genome and ensures the survival of future generations (Gartner et al., 2008; Setlow, 2006). In the absence of CmpA, cells run the risk of producing large numbers of spores that harbor mutations that may not confer the resistance properties required to protect the cell’s genome.

Why is it more beneficial to completely remove defective spores from a population, rather than allowing spores that harbor mutations, to persist? Sporulating cells employ a bet-hedging strategy whereby a fraction of the population does not initiate sporulation in order to retain the ability to rapidly respond to a return to favorable growth conditions (Veening et al., 2008). During continued favorable growth conditions, the selective pressure to maintain sporulation becomes relaxed, resulting in the enrichment of sporulation-defective cells

(Maughan et al., 2007; Sastalla et al., 2010). In the absence of the CmpA pathway, cells harboring mutations that diminish spore envelope assembly can complete sporulation and persist in the population. When these mutant cells resume vegetative growth, and eventually re-sporulate, a fraction of them may employ the bet-hedging strategy and avoid initiating sporulation. In this scenario, this group of non-sporulating cells has the capacity to quickly flourish, upon a sudden increase in nutrient availability, and out-compete the population of WT cells that initiate sporulation. Therefore, it is important for the population to actively remove cells that accumulate detrimental mutations. We propose that the CmpA pathway ensures that mutations diminishing the capacity to produce a robust spore do not become incorporated into the bacterium's "germ line" and ensures that faulty spores, which may be prone to accumulate additional mutations leading to the ultimate deterioration of the sporulation program, are removed by lysis.

Interestingly, the degradation of SpoIVA, which forms static polymers to encase the forespore, is reminiscent of the degradation of the nuclear lamins (static intermediate filaments that maintain the integrity of the nuclear envelope) during apoptosis in metazoans. While degradation of lamins is a feature of apoptosis, incorrect assembly of lamins to form the nuclear envelope can also induce apoptosis (Burke, 2001). Similarly, SpoIVA may not only be a target for degradation, but its incorrect assembly appears to induce CmpA-dependent cell lysis. Thus, the ability of morphogenetic proteins that serve to maintain the integrity of cellular envelopes to play these dual roles in regulated cell death appears to have arisen in evolutionarily and mechanistically distinct systems.

EXPERIMENTAL PROCEDURES

For a full explanation of experimental protocols, please see the Supplemental Experimental Procedures.

Strain construction

Strains are otherwise isogenic derivatives of *B. subtilis* PY79 (Youngman et al., 1984). Point mutant variants of *cmpA, cmpA-gfp, clpX* and *clpX-His*$_6$ were created using integration vectors containing the appropriate inserts as templates for Quikchange site-directed mutagenesis (Agilent). All plasmids were integrated into the *B. subtilis* chromosome by double recombination at the specified ectopic locus.

General methods

Sporulation efficiency was measured by inducing sporulation in Difco sporulation medium (DSM) for at least 24 h at 37°C and subjecting spores to heat treatment (80°C for 20 min) or lysozyme treatment (250 μg ml^{-1} for 1 h at 37°C). Cultures were then serially diluted and colony-forming units (cfu) that survived were determined and reported relative to the cfu obtained in a parallel culture of the WT PY79 strain. Viable spore counts were determined by first purifying spores using 30%–70% metrizoic acid density gradient centrifugation, then determining cfu ml^{-1} by serial dilution. PG was harvested from 1 ml cultures by acid hydrolysis and analyzed by HPLC; DPA was harvested from 5 ml cultures and analyzed by a colorimetric assay. Spontaneous suppressor mutations were identified by enriching for

mutants that grew after multiple rounds of sporulation and heat treatment followed by whole genome sequencing.

Microscopy

Cells were induced to sporulate by resuspension in SM medium (Sterlini and Mandelstam, 1969). When required, IPTG was added (1 mM final concentration) to induce expression of wild type or variants of *clpX* or *cmpA*. At various time points 1 ml of culture was harvested and resuspended in 100 µl PBS. 5 µl was spotted on a glass bottom culture dish (Mattek Corp.) and covered with a 1% agarose pad made with distilled water. Cells were viewed at 25°C with a DeltaVision Core microscope system (Applied Precision/GE Healthcare) equipped with a Photometrics CoolSnap HQ2 camera and an environmental chamber. Seventeen planes were acquired every 200 nm and the data were deconvolved using SoftWorx software as described previously (Eswaramoorthy et al., 2014).

Co-purification

Overnight cultures were grown in CH media and induced to sporulate in 20 ml resuspension medium. IPTG (1 mM final concentration) was added to induce expression of tagged or untagged versions of WT and mutant CmpA and ClpX 2 h after resuspension. Cells were harvested and protoplasted in protoplast buffer (0.5 M sucrose, 20 mM $MgCl_2$, 10 mM potassium phosphate at pH 6.8, 0.1 mg ml^{-1} lysozyme) for 25 min at 37°C. Protoplasts were collected by centrifugation and resuspended in 1 ml of ice cold 0.5X PD buffer (Kim et al., 2001) without ATP regenerating system (hereafter referred to as 0.5X PD buffer). Phenylmethylsulfonyl fluoride (1mM final concentration) was added to cell lysate and cell debris was removed by centrifugation. The supernatant was collected and incubated with Ni-NTA agarose beads (Qiagen) equilibrated in 0.5X PD buffer for 10 min at 4°C with inversion. Beads were washed with 0.5X PD buffer containing 20mM imidazole. Bound proteins were eluted with 250 µl of 0.5X PD buffer containing 250mM imidazole. Fractions were analyzed by immunoblotting using rabbit antisera raised against purified *E. coli* ClpX (gift from Sue Wickner), GFP, or SpoIVA.

Cell lysate harvesting

Overnight cultures were grown in CH medium and induced to sporulate by the resuspension method (described above). 1 ml of culture was harvested at various time points. Cells were harvested and protoplasted as described above. Protoplasts were resuspended in 500 µl 5% tricholoroacetic acid (TCA) to lyse cells and precipitate proteins. After incubation on ice for 15 min, precipitate was collected by centrifugation and washed three times with 1 ml acetone. Precipitated pellet was air-dried overnight at room temperature, then resuspended in 300 µl 1× LDS NuPAGE Buffer (Invitrogen) and heated at 55°C f or 10 min with shaking. Fractions were analyzed by immunoblotting using rabbit antisera raised against SpoIVA or σ^A.

Supplementary Material

Refer to Web version on PubMed Central for supplementary material.

Acknowledgments

We thank V. Bliskovsky (Genomics Core facility, NCI) for whole genome sequencing of spontaneous suppressors; P. Setlow, R. Losick, D. Kearns, S. Ebmeier, and D. Ziegler (BGSC) for strains; S. Wickner for *E. coli* ClpX antiserum; S. Gottesman, S. Wickner, M. Maurizi, G. Storz, M. Lichten, and Y.-S. Lee for discussion; and A. Hitchcock-Camp and C. Ellermeier for comments on the manuscript. This work was funded by NIH grant AI088298 (DLP) and the Intramural Research Program of the National Institutes of Health, National Cancer Institute, Center for Cancer Research (KSR).

References

Baker TA, Sauer RT. ClpXP, an ATP-powered unfolding and protein-degradation machine. Biochim Biophys Acta. 2012; 1823:15–28. [PubMed: 21736903]

Battesti A, Gottesman S. Roles of adaptor proteins in regulation of bacterial proteolysis. Curr Opin Microbiol. 2013; 16:140–147. [PubMed: 23375660]

Bejerano-Sagie M, Oppenheimer-Shaanan Y, Berlatzky I, Rouvinski A, Meyerovich M, Ben-Yehuda S. A checkpoint protein that scans the chromosome for damage at the start of sporulation in Bacillus subtilis. Cell. 2006; 125:679–690. [PubMed: 16713562]

Bos J, Yakhnina AA, Gitai Z. BapE DNA endonuclease induces an apoptotic-like response to DNA damage in *Caulobacter*. Proc Natl Acad Sci U S A. 2012; 109:18096–18101. [PubMed: 23074244]

Burke B. Lamins and apoptosis: a two-way street? J Cell Biol. 2001; 153:F5–7. [PubMed: 11331313]

Burkholder WF, Kurtser I, Grossman AD. Replication initiation proteins regulate a developmental checkpoint in Bacillus subtilis. Cell. 2001; 104:269–279. [PubMed: 11207367]

Castaing JP, Lee S, Anantharaman V, Ravilious GE, Aravind L, Ramamurthi KS. An autoinhibitory conformation of the *Bacillus subtilis* spore coat protein SpoIVA prevents its premature ATP-independent aggregation. FEMS Microbiol Lett. 2014; 358:145–153. [PubMed: 24810258]

Castaing JP, Nagy A, Anantharaman V, Aravind L, Ramamurthi KS. ATP hydrolysis by a domain related to translation factor GTPases drives polymerization of a static bacterial morphogenetic protein. Proc Natl Acad Sci U S A. 2013; 110:E151–160. [PubMed: 23267091]

Catalano FA, Meador-Parton J, Popham DL, Driks A. Amino acids in the *Bacillus subtilis* morphogenetic protein SpoIVA with roles in spore coat and cortex formation. J Bacteriol. 2001; 183:1645–1654. [PubMed: 11160095]

Dwyer DJ, Camacho DM, Kohanski MA, Callura JM, Collins JJ. Antibiotic-induced bacterial cell death exhibits physiological and biochemical hallmarks of apoptosis. Mol Cell. 2012; 46:561–572. [PubMed: 22633370]

Ebmeier SE, Tan IS, Clapham KR, Ramamurthi KS. Small proteins link coat and cortex assembly during sporulation in *Bacillus subtilis*. Mol Microbiol. 2012; 84:682–696. [PubMed: 22463703]

Eswaramoorthy P, Winter PW, Wawrzusin P, York AG, Shroff H, Ramamurthi KS. Asymmetric division and differential gene expression during a bacterial developmental program requires DivIVA. PLoS Genet. 2014; 10:e1004526. [PubMed: 25101664]

Fiche JB, Cattoni DI, Diekmann N, Langerak JM, Clerte C, Royer CA, Margeat E, Doan T, Nollmann M. Recruitment, assembly, and molecular architecture of the SpoIIIE DNA pump revealed by superresolution microscopy. PLoS Biol. 2013; 11:e1001557. [PubMed: 23667326]

Galluzzi L, Vitale I, Abrams JM, Alnemri ES, Baehrecke EH, Blagosklonny MV, Dawson TM, Dawson VL, El-Deiry WS, Fulda S, et al. Molecular definitions of cell death subroutines: recommendations of the Nomenclature Committee on Cell Death 2012. Cell Death Differ. 2012; 19:107–120. [PubMed: 21760595]

Gartner A, Boag PR, Blackwell TK. Germline survival and apoptosis. WormBook. 2008:1–20. [PubMed: 18781708]

Gill RL Jr, Castaing JP, Hsin J, Tan IS, Wang X, Huang KC, Tian F, Ramamurthi KS. Structural basis for the geometry-driven localization of a small protein. Proc Natl Acad Sci U S A. 2015; 112:E1908–1915. [PubMed: 25825747]

Gottesman S. Proteases and their targets in *Escherichia coli*. Annu Rev Genet. 1996; 30:465–506. [PubMed: 8982462]

Gottesman S, Clark WP, de Crecy-Lagard V, Maurizi MR. ClpX, an alternative subunit for the ATP-dependent Clp protease of *Escherichia coli*. Sequence and in vivo activities. J Biol Chem. 1993; 268:22618–22626. [PubMed: 8226770]

Hacker G. Is there, and should there be, apoptosis in bacteria? Microbes Infect. 2013; 15:640–644. [PubMed: 23747737]

Hartwell LH, Weinert TA. Checkpoints: controls that ensure the order of cell cycle events. Science. 1989; 246:629–634. [PubMed: 2683079]

Heffron JD, Orsburn B, Popham DL. Roles of germination-specific lytic enzymes CwlJ and SleB in *Bacillus anthracis*. J Bacteriol. 2009; 191:2237–2247. [PubMed: 19181808]

Henriques AO, Moran CP Jr. Structure, assembly, and function of the spore surface layers. Annu Rev Microbiol. 2007; 61:555–588. [PubMed: 18035610]

Higgins D, Dworkin J. Recent progress in *Bacillus subtilis* sporulation. FEMS Microbiol Rev. 2012; 36:131–148. [PubMed: 22091839]

Holtje JV. Growth of the stress-bearing and shape-maintaining murein sacculus of *Escherichia coli*. Microbiol Mol Biol Rev. 1998; 62:181–203. [PubMed: 9529891]

Imae Y, Strominger JL. Relationship between cortex content and properties of *Bacillus sphaericus* spores. J Bacteriol. 1976; 126:907–913. [PubMed: 944183]

Kim YI, Levchenko I, Fraczkowska K, Woodruff RV, Sauer RT, Baker TA. Molecular determinants of complex formation between Clp/Hsp100 ATPases and the ClpP peptidase. Nat Struct Biol. 2001; 8:230–233. [PubMed: 11224567]

Kunkel B, Losick R, Stragier P. The *Bacillus subtilis* gene for the development transcription factor sigma K is generated by excision of a dispensable DNA element containing a sporulation recombinase gene. Genes Dev. 1990; 4:525–535. [PubMed: 2163341]

Lau J, Hernandez-Alicea L, Vass RH, Chien P. A Phosphosignaling Adaptor Primes the AAA+ Protease ClpXP to Drive Cell Cycle-Regulated Proteolysis. Mol Cell. 2015; 59:104–116. [PubMed: 26073542]

Leggett MJ, McDonnell G, Denyer SP, Setlow P, Maillard JY. Bacterial spore structures and their protective role in biocide resistance. J Appl Microbiol. 2012; 113:485–498. [PubMed: 22574673]

Levin PA, Fan N, Ricca E, Driks A, Losick R, Cutting S. An unusually small gene required for sporulation by *Bacillus subtilis*. Mol Microbiol. 1993; 9:761–771. [PubMed: 8231808]

Liu J, Cosby WM, Zuber P. Role of lon and ClpX in the post-translational regulation of a sigma subunit of RNA polymerase required for cellular differentiation in *Bacillus subtilis*. Mol Microbiol. 1999; 33:415–428. [PubMed: 10411757]

Maughan H, Masel J, Birky CW Jr, Nicholson WL. The roles of mutation accumulation and selection in loss of sporulation in experimental populations of *Bacillus subtilis*. Genetics. 2007; 177:937–948. [PubMed: 17720926]

McFarland KA, Dolben EL, LeRoux M, Kambara TK, Ramsey KM, Kirkpatrick RL, Mougous JD, Hogan DA, Dove SL. A self-lysis pathway that enhances the virulence of a pathogenic bacterium. Proc Natl Acad Sci U S A. 2015; 112:8433–8438. [PubMed: 26100878]

McKenney PT, Driks A, Eichenberger P. The *Bacillus subtilis* endospore: assembly and functions of the multilayered coat. Nat Rev Microbiol. 2013; 11:33–44. [PubMed: 23202530]

McKenney PT, Driks A, Eskandarian HA, Grabowski P, Guberman J, Wang KH, Gitai Z, Eichenberger P. A distance-weighted interaction map reveals a previously uncharacterized layer of the *Bacillus subtilis* spore coat. Curr Biol. 2010; 20:934–938. [PubMed: 20451384]

Paidhungat M, Setlow B, Driks A, Setlow P. Characterization of spores of *Bacillus subtilis* which lack dipicolinic acid. J Bacteriol. 2000; 182:5505–5512. [PubMed: 10986255]

Popham DL, Helin J, Costello CE, Setlow P. Analysis of the peptidoglycan structure of Bacillus subtilis endospores. J Bacteriol. 1996; 178:6451–6458. [PubMed: 8932300]

Price KD, Losick R. A four-dimensional view of assembly of a morphogenetic protein during sporulation in *Bacillus subtilis*. J Bacteriol. 1999; 181:781–790. [PubMed: 9922240]

Ramamurthi KS, Clapham KR, Losick R. Peptide anchoring spore coat assembly to the outer forespore membrane in *Bacillus subtilis*. Mol Microbiol. 2006; 62:1547–1557. [PubMed: 17427285]

Ramamurthi KS, Lecuyer S, Stone HA, Losick R. Geometric cue for protein localization in a bacterium. Science. 2009; 323:1354–1357. [PubMed: 19265022]

Ramamurthi KS, Losick R. ATP-driven self-assembly of a morphogenetic protein in *Bacillus subtilis*. Mol Cell. 2008; 31:406–414. [PubMed: 18691972]

Roels S, Driks A, Losick R. Characterization of spoIVA, a sporulation gene involved in coat morphogenesis in *Bacillus subtilis*. J Bacteriol. 1992; 174:575–585. [PubMed: 1729246]

Sastalla I, Rosovitz MJ, Leppla SH. Accidental selection and intentional restoration of sporulation-deficient *Bacillus anthracis* mutants. Appl Environ Microbiol. 2010; 76:6318–6321. [PubMed: 20639373]

Schirmer EC, Glover JR, Singer MA, Lindquist S. HSP100/Clp proteins: a common mechanism explains diverse functions. Trends Biochem Sci. 1996; 21:289–296. [PubMed: 8772382]

Setlow P. Spores of *Bacillus subtilis*: their resistance to and killing by radiation, heat and chemicals. J Appl Microbiol. 2006; 101:514–525. [PubMed: 16907802]

Smith TJ, Foster SJ. Characterization of the involvement of two compensatory autolysins in mother cell lysis during sporulation of *Bacillus subtilis* 168. J Bacteriol. 1995; 177:3855–3862. [PubMed: 7601853]

Sterlini JM, Mandelstam J. Commitment to sporulation in *Bacillus subtilis* and its relationship to development of actinomycin resistance. Biochem J. 1969; 113:29–37. [PubMed: 4185146]

Tan IS, Ramamurthi KS. Spore formation in *Bacillus subtilis*. Environ Microbiol Rep. 2014; 6:212–225. [PubMed: 24983526]

Vasudevan P, Weaver A, Reichert ED, Linnstaedt SD, Popham DL. Spore cortex formation in *Bacillus subtilis* is regulated by accumulation of peptidoglycan precursors under the control of sigma K. Mol Microbiol. 2007; 65:1582–1594. [PubMed: 17714441]

Veening JW, Murray H, Errington J. A mechanism for cell cycle regulation of sporulation initiation in Bacillus subtilis. Genes Dev. 2009; 23:1959–1970. [PubMed: 19684115]

Veening JW, Stewart EJ, Berngruber TW, Taddei F, Kuipers OP, Hamoen LW. Bet-hedging and epigenetic inheritance in bacterial cell development. Proc Natl Acad Sci U S A. 2008; 105:4393–4398. [PubMed: 18326026]

Wojtkowiak D, Georgopoulos C, Zylicz M. Isolation and characterization of ClpX, a new ATP-dependent specificity component of the Clp protease of *Escherichia coli*. J Biol Chem. 1993; 268:22609–22617. [PubMed: 8226769]

Wojtyra UA, Thibault G, Tuite A, Houry WA. The N-terminal zinc binding domain of ClpX is a dimerization domain that modulates the chaperone function. J Biol Chem. 2003; 278:48981–48990. [PubMed: 12937164]

Wu IL, Narayan K, Castaing JP, Tian F, Subramaniam S, Ramamurthi KS. A versatile nano display platform from bacterial spore coat proteins. Nat Commun. 2015; 6:6777. [PubMed: 25854653]

Youngman P, Perkins JB, Losick R. Construction of a cloning site near one end of Tn917 into which foreign DNA may be inserted without affecting transposition in *Bacillus subtilis* or expression of the transposon-borne *erm* gene. Plasmid. 1984; 12:1–9. [PubMed: 6093169]

Zhou Y, Gottesman S, Hoskins JR, Maurizi MR, Wickner S. The RssB response regulator directly targets sigma(S) for degradation by ClpXP. Genes Dev. 2001; 15:627–637. [PubMed: 11238382]

HIGHLIGHTS

- During sporulation misassembly of the spore envelope causes CmpA-mediated lysis
- CmpA is a ClpXP adaptor for degradation of the morphogenetic protein SpoIVA
- The CmpA pathway helps ensure evolutionary maintenance of the sporulation program

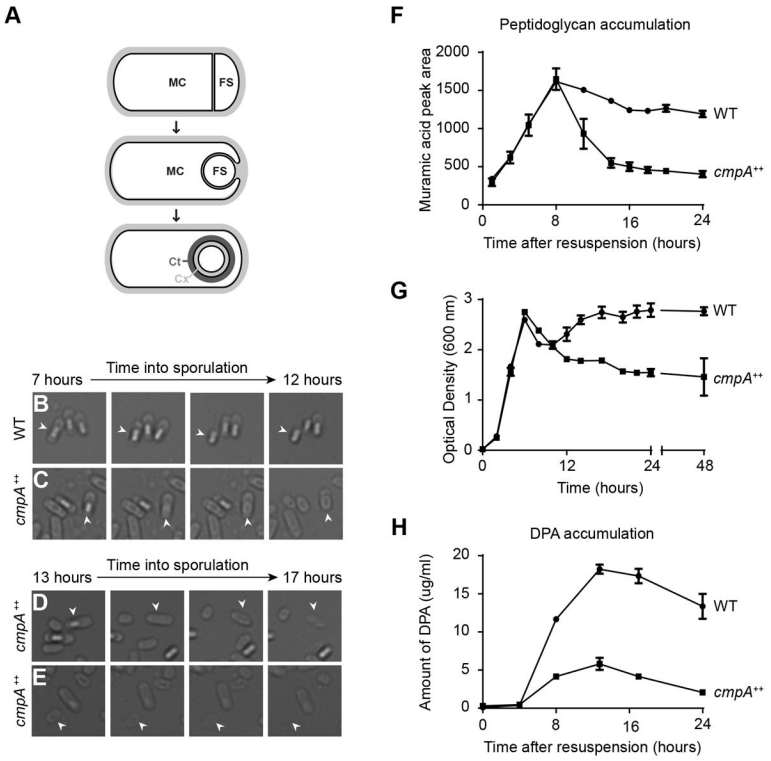

Figure 1.

Overexpression of *cmpA* causes cell lysis and defects in cortex maintenance. (A) Schematic of sporulation in *Bacillus subtilis*. Asymmetric division (top) results in the formation of the larger mother cell (MC) and smaller forespore (FS) compartments, which are genetically identical. Next, the mother cell engulfs the forespore (middle). Eventually, the forespore resides in the mother cell cytosol (bottom). The forespore is encased in two concentric shells: the proteinaceous coat (Ct, dark gray), and the cortex (Cx, light gray), made of a specialized peptidoglycan. Membranes are depicted in black; cell wall material is depicted in light gray. (BE) Time-lapse microscopy of sporulating WT (C; strain PY79) and *cmpA* overexpressing (D–F; IT478) cells. Time after induction of sporulation is indicated above. Fate of phase bright forespores in WT (B) and *cmpA* overexpressing (C) cells. Fate of (D) phase gray forespores in *cmpA* overexpressing cells while still in the mother cell, or phase gray spores (E) after release into the medium. Arrowheads indicate phase gray forespore or released spore. (F) Accumulation of peptidoglycan during sporulation in WT (●; PY79) and *cmpA* overexpressing (■; IT478) cells. (G) Growth curves, as measured by optical density of the cultures grown in sporulation media (DSM), of WT (●; PY79) and *cmpA* overexpressing (■; IT478) strains. (H) Accumulation of dipicolinic acid (DPA) during sporulation in WT (●; PY79) and *cmpA* overexpressing (■ IT478) cells. Symbols represent mean values obtained from three independent measurements; error bars represent standard error of the mean. Strain genotypes are listed in Table S8. See also Figure S1 and Table S1–S2.

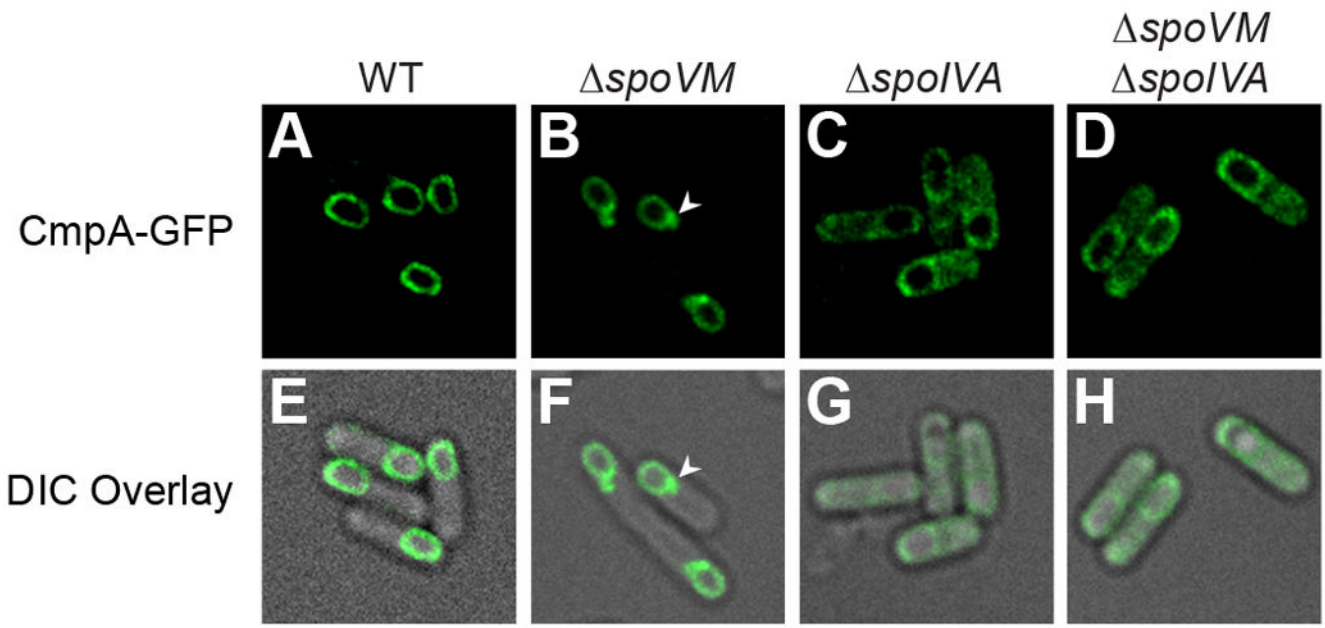

Figure 2.

CmpA-GFP localization is dependent on *spoIVA*. (A–D) Localization of CmpA-GFP in WT (A; SE364), Δ*spoVM* (B; IT86), Δ*spoIVA* (C; IT114) and Δ*spoVM* Δ*spoIVA* (D; IT113) cells. Arrowheads (B, F) indicate mislocalized focus of CmpA-GFP. (E–H) Overlay of DIC and GFP fluorescence from A–D, respectively. See also Table S3.

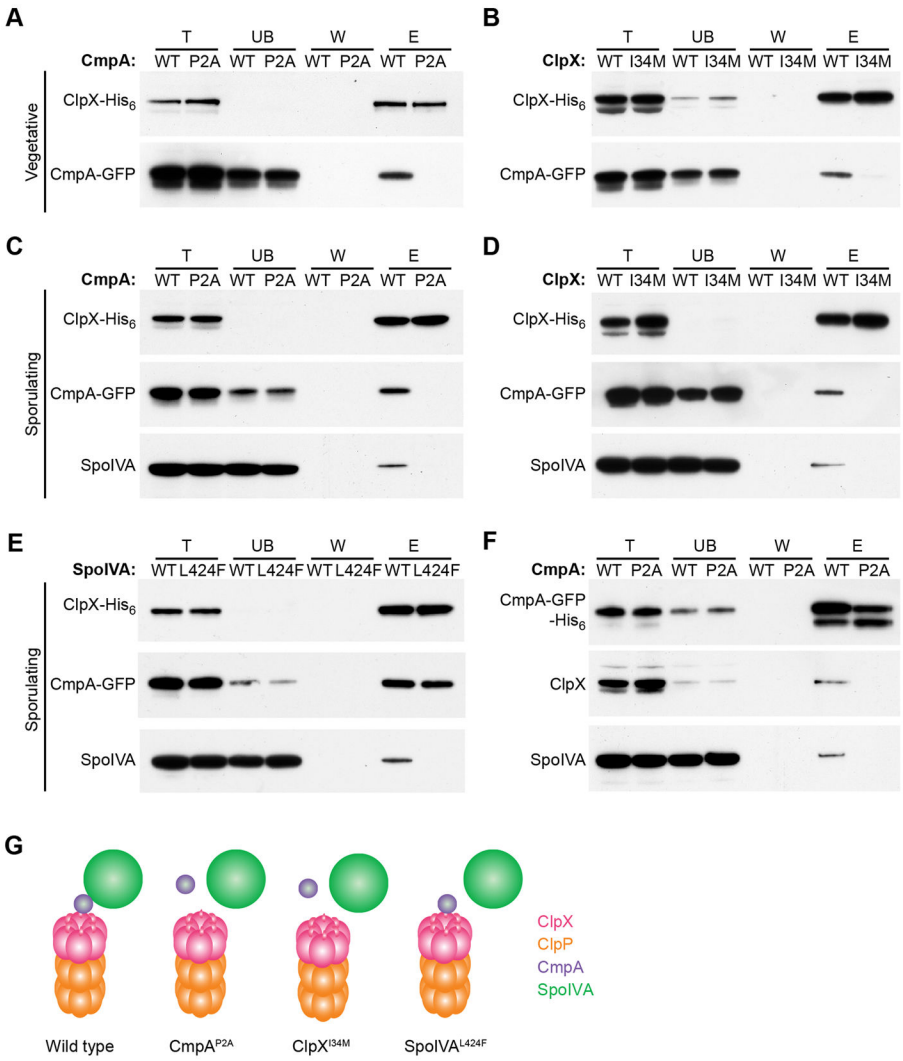

Figure 3.

ClpX, CmpA and SpoIVA form a complex. (A–B) Extracts of vegetative *B. subtilis* producing CmpA-GFP and ClpX-His$_6$ (A; IT735) or ClpX^{I34M}-His$_6$ (B; T751) were applied to a Ni^{2+}-agarose affinity column and eluted. The presence of ClpX and CmpA-GFP in the total (T), unbound (UB), wash (W), or eluate (E) fractions was monitored by immunoblotting. (C–F) Extracts of sporulating *B. subtilis* producing CmpA^{P2A}-GFP and ClpX-His$_6$ (C; IT760); ClpX^{I34M}-His$_6$ and CmpA-GFP (D; IT751); ClpX-His$_6$, CmpA-GFP, and SpoIVA^{L424F} (E; IT818); or CmpA-GFP-His$_6$ (F; IT784) were applied to a Ni^{2+}-agarose affinity chromatography and eluted. The presence of ClpX, CmpA-GFP, and SpoIVA were monitored in each fraction by immunoblotting. (G) Schematic summarizing the interactions between variants of ClpX, CmpA, and SpoIVA (ClpX, pink; ClpP, orange; CmpA, purple; SpoIVA, green). See also Figure S2 and Table S4–S6.

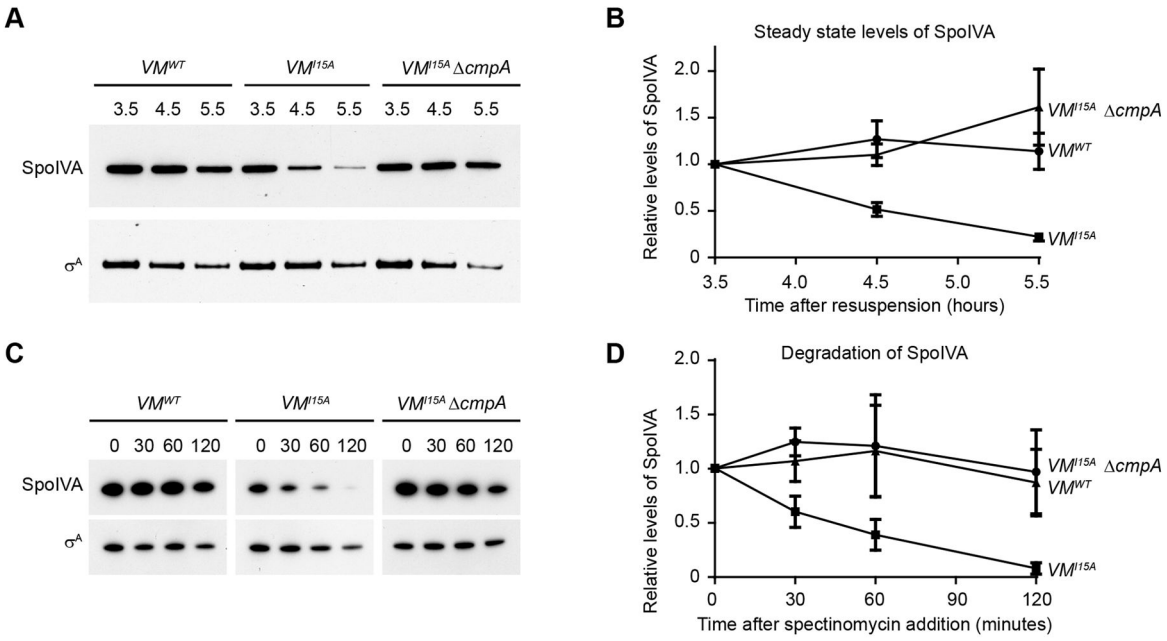

Figure 4.

SpoIVA is degraded in a *cmpA* dependent manner in the *spoVM*^{I15A} mutant. (A) Cell extracts were prepared from sporulating cells of Δ*spoIVA* (KP73), or strains harboring WT *spoVM* (KR103), *spoVM*^{II15A} (KR322), or *spoVM*^{II15} Δ*cmpA* (SE181) at times (h) indicated after induction of sporulation. SpoIVA and, as a control, σ^A were detected by immunoblotting. (B) Quantification of SpoIVA band intensities of each strain in (A) relative to σ^A levels at each time point and represented as a fraction compared to the level at $t_{3.5}$ (●, *spoVM*^{WT}; ■, *spoVM*^{II15A}; ▲, *spoVM*^{II15} △*cmpA*). (C) Strains KR103, KR322, and SE181 were induced to sporulate. At $t_{4.5}$, spectinomycin (200 μg ml^{-1}) was added to inhibit translation and cell extracts were prepared from aliquots taken at the times (min) indicated. SpoIVA and σ^A were detected by immunoblotting. (D) Quantification of SpoIVA band intensities in (C) relative to σ^A levels at each time point and represented as a fraction compared to the level at t_0 after addition of spectinomycin (●, *spoVM*^{WT};■, *spoVM*^{II15A}; ▲, *spoVM*^{II15} △*cmpA*). Symbols represent mean values obtained from four (B) or three (D) independent measurements; error bars represent standard error of the mean.

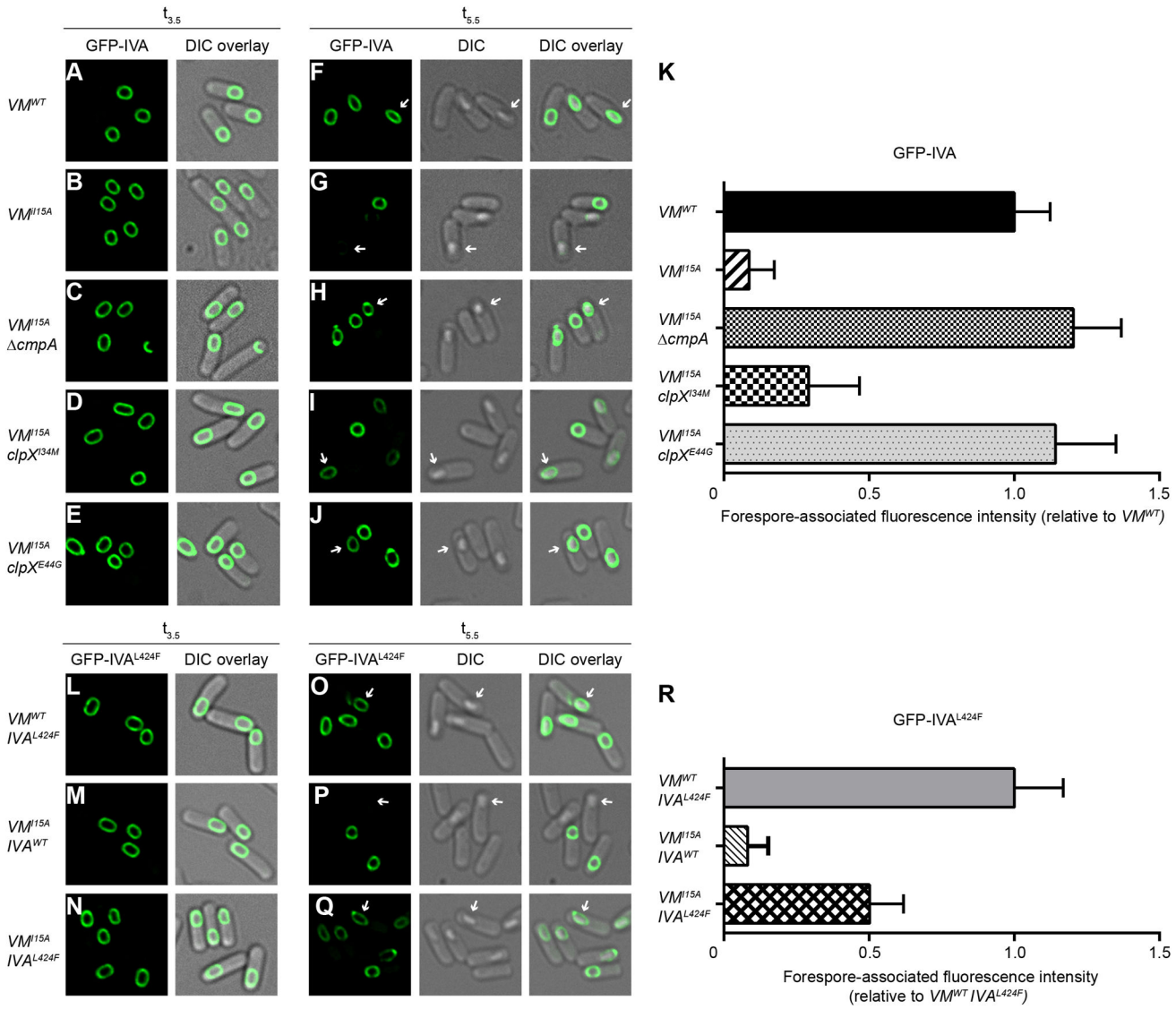

Figure 5.

CmpA-dependent degradation of GFP-SpoIVA in sporangia harboring *spoVM*^{I15A} that elaborate phase bright forespores. (A–J) GFP-SpoIVA in cells harboring *spoVM*^{WT} (A and F, KR165) *spoVM*^{I15A} (B and G, KRC77), *spoVM*^{I15A} Δ*cmpA* (C and H, IT839), *spoVM*^{I15A} *clpX*^{I34M} (D and I, IT884) or *spoVM*^{I15A} *clpX*^{E44G} (E and J, IT883) at $t_{3.5}$ (A–E) and $t_{5.5}$ (F–J) after induction of sporulation. (K) Quantification of GFP-SpoIVA fluorescence in strains shown in (A–J). (L–Q) GFP-SpoIVA^{L424F} in cells harboring *spoVM*^{WT} *spoIVA*^{L424F}(L and O, IT869), *spoVM*^{I15A} *spoIVA*^{WT} (M and P, KRC77) or *spoVM*^{I15A} *spoIVA*^{L424F} (N and Q, IT852) at $t_{3.5}$ (L–N) and $t_{5.5}$ (O–Q) after induction of sporulation. (R) Quantification of GFP-SpoIVA^{L424F} forespore-associated fluorescence in strains shown in (L–Q). All bars represent mean values of >80 phase bright forespores; error bars represent standard deviation. Arrows indicate a phase bright forespore. See also Figure S3.

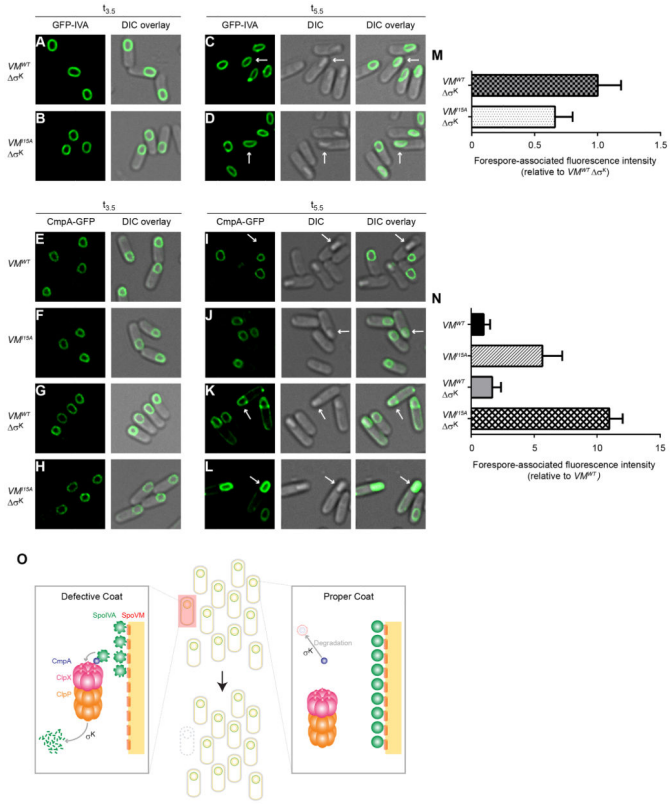

Figure 6.

Additional factor(s) under σ^K control are required for SpoIVA and CmpA-GFP degradation. (A–D) GFP-SpoIVA in cells harboring *spoVM*^{WT} Δσ^K (A and C, IT891) or *spoVM*^{I15A} $^3\sigma^K$ (B and D, IT892) at $t_{3.5}$ (A–B) or $t_{5.5}$ (C–D) after induction of sporulation. (E–L) CmpA-GFP in cells harboring *spoVM*^{WT}(E and I, IT897), *spoVM*^{I15A} (F and J, IT896), *spoVM*^{WT} $^3\sigma^K$ (G and K, IT904) or *spoVM*^{I15A} $^3\sigma^K$ (H and L, IT903) at $t_{3.5}$ (E–H) or $t_{5.5}$ (I–L) after induction of sporulation. Arrows indicate a phase bright forespore. (M–N) Quantification of forespore-associated GFP fluorescence intensities shown in (C–D) and (I–L), respectively. All bars represent mean values of 14–101 phase bright forespores; error bars represent standard deviation. See also Figure S4 and Table S7. (O) Model of the CmpA-mediated regulated cell death pathway. Depicted is a population of sporulating *B. subtilis* cells (center, top) in which a single cell has elaborated a defective spore envelope (highlighted in red) and, as a consequence, is removed from the population by cell lysis (center, bottom). Left: the CmpA pathway in a cell elaborating a defective spore envelope. CmpA persists in this cell and acts as an adaptor of ClpXP to mediate degradation of SpoIVA in a σ^K-dependent manner. Right: in cells that successfully initiate spore envelope assembly, CmpA is degraded upon activation of σ^K and, in the absence of SpoIVA degradation, the sporulation program proceeds. SpoIVA, green; SpoVM, red; CmpA, purple; ClpX, pink; ClpP, orange.

Table 1

Sporulation efficiencies (as measured by heat or lysozyme resistance) of *spoVM* and *spoIVA* mutants with and without deletion of *cmpA.* Standard deviation from mean is reported in parentheses (n=3).

Strain[a]	Mutation	*cmpA*	Sporulation Efficiency (relative to WT)	
			Heat Resistance	Lysozyme Resistance
A	WT	-	1	1
B	*spoVM*^{K2A}		0.01 (0.007)	0.007 (0.003)
C	*spoVM*^{K2A}	Δ	0.25 (0.05)	0.47 (0.03)
D	*spoVM*^{I15A}		5×10^{-6} (1.7×10^{-6})	1.8×10^{-6} (1.1×10^{-6})
E	*spoVM*^{I15A}	Δ	0.16 (0.09)	0.05 (0.01)
F	*spoIVA*^{K30A}		3.8×10^{-4} (1.7×10^{-4})	3×10^{-4} (3.2×10^{-4})
G	*spoIVA*^{K30A}	Δ	0.08 (0.01)	0.03 (0.02)
H	*spoIVA*$^{T70A\text{-}T71A}$		5.8×10^{-6} (3×10^{-6})	2×10^{-6} (1×10^{-6})
I	*spoIVA*$^{T70A\text{-}T71A}$	Δ	0.02 (0.01)	0.002 (7×10^{-4})
J	Δ*spoIVA*		$<10^{-8}$	$<10^{-8}$
K	Δ*spoIVA*	Δ	$<10^{-8}$	ND

[a]Strain A: PY79; B: KRC102; C:IT102; D: KR322; E:SE181; F:KR367; G:IT880; H: JPC221; I: IT882; J: KP73; K: IT895. Genotypes are listed in Table S9. ND, not determined.